One-dimensional β–Ga_2O_3 nanostructures on sapphire (0001): Low-temperature epitaxial nanowires and high-temperature nanorod bundles

Ko-Wei Chang
Department of Chemical Engineering, National Cheng Kung University, Tainan, Taiwan, Republic of China
Jih-Jen Wu[a)]
Department of Chemical Engineering, National Cheng Kung University, Tainan, Taiwan, Republic of China; and Center for Micro/Nano Technology Research, National Cheng Kung University, Tainan, Taiwan, Republic of China

(Received 27 April 2005; accepted 1 September 2005)

Well-aligned Ga_2O_3 nanowires were formed on the sapphire (0001) substrates at temperatures of 650–450 °C using a single precursor of gallium acetylacetonate via a vapor-liquid-solid (VLS) method. Structural analyses reveal that the well-aligned Ga_2O_3 nanowires are expitaxially grown on the sapphire (0001) with Ga_2O_3/ sapphire orientational relationship $[\bar{2}01] \| [0001]$ and $[2\bar{1}1] \| [11\bar{2}0]$. In addition, formation of the flowerlike Ga_2O_3 nanorod bundles at a temperature of 750 °C via the vapor-solid (VS) mechanism was also demonstrated. Instead of being catalysts in the VLS method, the Au nanoparticles are proposed to play a role in sinking the Ga vapor for forming the nuclei of Ga_2O_3 nanorods in the VS method.

I. INTRODUCTION

Because monoclinic Ga_2O_3 (β–Ga_2O_3) exhibits a wide band gap (Eg = 4.9 eV) with potential application in optoelectronic devices and high-temperature stable sensors,[1,2] β–Ga_2O_3 nanowires have been synthesized by various high-temperature (higher than 780 °C) methods, including the arc-discharge method,[3,4] vapor-liquid-solid (VLS) method,[5,6] carbothermal reduction,[7,8] thermal oxidation[9,10] via the vapor-solid (VS) process, and so on. In addition to nanowires, Ga_2O_3 nanobelt (nanoribbons)[9,11–13] and nanosheets[9,11,12] have also been demonstrated via a thermal oxidation method. Such high temperature is unavoidable for using gallium sources with high melting points such as Ga_2O_3, GaN and GaAs in those processes. However, the formation of well-ordered single crystalline nanowires with controlled crystal orientation on the substrates at lower temperatures is needed for application to nanoscale devices. Recently, we have reported the growth of the well-aligned Ga_2O_3 nanowires on sapphire (0001) substrate at a temperature of 550 °C.[14] A single precursor of gallium acetylacetonate with a low decomposition temperature (~196 °C) was used as the reactant for the Ga_2O_3 nanowires growth via the VLS method. The low decomposition temperature (~196 °C) of the organometallic source of gallium acetylacetonate can provide sufficient Ga and O vapors for the Ga_2O_3 nanowires growth by employing a two-temperature-zone furnace. The concentrations of Ga and O vapors can be controlled by the temperature of the low-temperature zone, which is independent of the temperature for Ga_2O_3 nanowires growth in the second zone.[14] Here, we report the epitaxial growth of the Ga_2O_3 nanowires on sapphire (0001) substrate at a temperature of 450 °C in a three-temperature-zone furnace. Formation of the flowerlike nanorod bundles at a temperature of 750 °C via the vapor-solid (VS) mechanism is also demonstrated.

II. EXPERIMENTAL

The one-dimensional (1D) Ga_2O_3 nanostructures were synthesized on Au pre-coated substrates. All substrates after being cleaned were coated with a 1-nm-thick Au layer using an e-beam evaporator. The Ga and O sources, gallium acetylacetonate [$(CH_3COCHCOCH_3)_3Ga$, Aldrich, 99.99%], placed on a cleaned Pyrex glass container was loaded into the low-temperature zone of the furnace, which was controlled to be 185 °C to vaporize the solid reactant. In addition to the N_2 main flow, a N_2 line [so-called N_2(Ga)] separated from the main N_2 stream was connected to the Pyrex glass to carry sufficient Ga and O sources to the high-temperature zone. The

---

[a)] Address all correspondence to this author.
e-mail: wujj@mail.ncku.edu.tw
DOI: 10.1557/JMR.2005.0417

pressure for the nanowire growth was set at 100 Torr. Two methods for growth of 1D Ga_2O_3 nanostructures in this study are described in the following subsections.

A. Growth method I

Formation of the 1D Ga_2O_3 nanostructures was conducted in a two-temperature-zone furnace, as shown in Fig. 1(a). The Pyrex glass container for precursors was placed at the low-temperature zone, and the substrate was loaded at the center of the high-temperature zone, set at 450–750 °C.

B. Growth method II

Formation of the 1D Ga_2O_3 nanowires was conducted in a three-temperature-zone furnace, as show in Fig. 1(b). The first zone was for vaporizing the gallium acetylacetonate. The second zone was set to be 550 °C for acetylacetonate precursor further pyrolysis, and the substrates were loaded in the third-zone region with a temperature of 450 °C.

The morphology and size distribution of as-deposited material were examined using scanning electron microscopy (SEM; JEOL JSM-7000F and Philips XL-40 FE-SEM). The crystal structures of the nanowires were investigated using x-ray diffraction (XRD, Rigaku) and

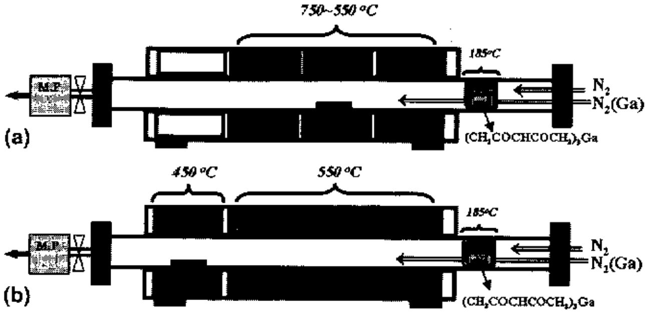

FIG. 1. Schematic diagrams of (a) the two-temperature-zone furnace and (b) the three-temperature-zone furnace.

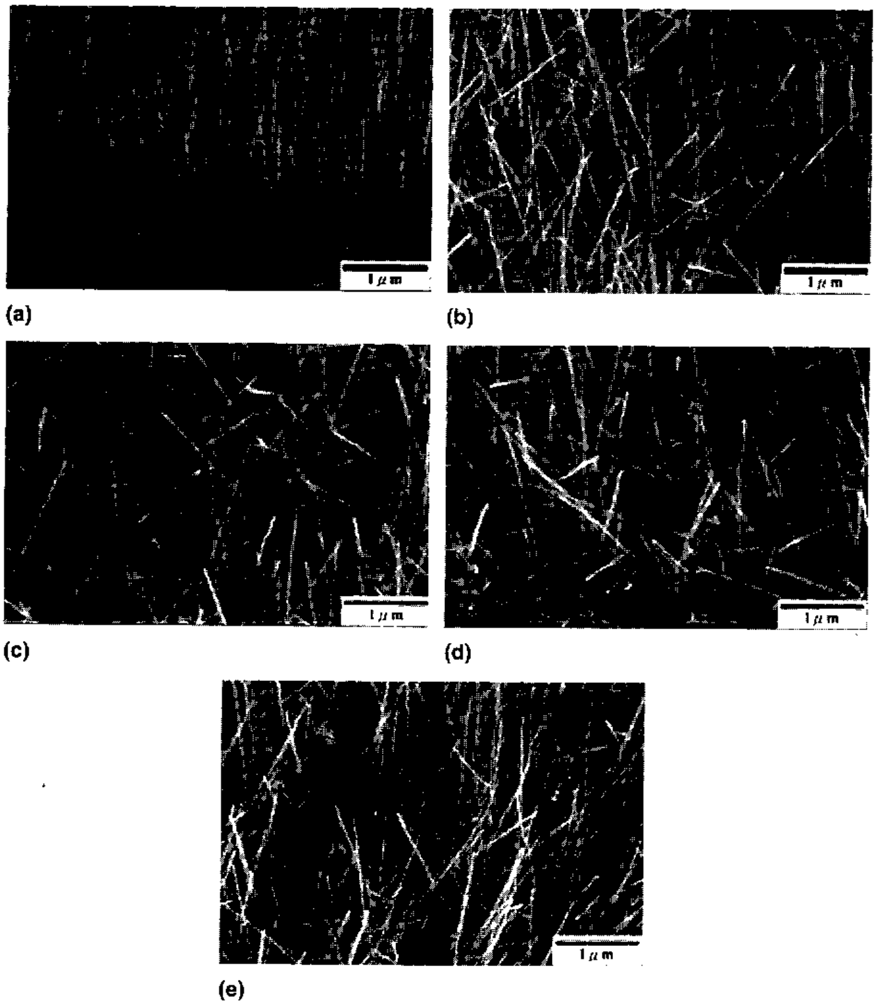

FIG. 2. Field-emission scanning electron microscopy (FE-SEM) images of Ga_2O_3 nanowires grown on (a) sapphire (0001), (b) Si (100), (c) sapphire (11$\bar{2}$0), (d) MgO (100), and (e) fused silica substrates at a temperature of 650 °C.

transmission electron microscopy (TEM; JEOL 2010 and JEOL 3010).

III. RESULTS AND DISCUSSION

Growth of the Ga_2O_3 nanowires was conducted at 650 °C on five types of materials, including sapphire (0001), sapphire (11$\bar{2}$0), Si (100), MgO (100), and fused silica, to study the effects of substrate materials on the nanowire growth in a two-temperature-zone furnace [growth method I, as shown in Fig. 1(a)]. The substrates were pre-coated with a 1-nm-thick Au layer as catalyst for the VLS mechanism. Figure 2(a) shows that well-aligned nanowires formed on sapphire (0001) substrate. However, as shown in Figs. 2(b)–2(e), the aligned features are not observed on the nanowires grown on the other substrates under the same growth conditions. The powder-diffraction-mode XRD patterns of these nanowires were taken to investigate the crystal structures and the well-aligned characteristic of the nanowires. Pattern I in Fig. 3 reveals that in addition to the (0001) sapphire and (300) Au_7Ga_2 diffraction peaks corresponding to the substrate and the catalyst, respectively, the other two peaks are indexed as ($\bar{4}$02) and ($\bar{6}$03) diffraction peaks of the β–Ga_2O_3 structure, demonstrating the nanowires grown on the sapphire (0001) substrate are preferentially oriented in the [$\bar{2}$01] direction. Patterns II–V in Fig. 3 show that the diffraction peaks apart from the one ascribed to the substrate can be indexed to those of β–Ga_2O_3. However, preferentially oriented Ga_2O_3 nanowires on the sapphire (11$\bar{2}$0), Si (100), MgO (100), and fused silica substrates were not obtained.

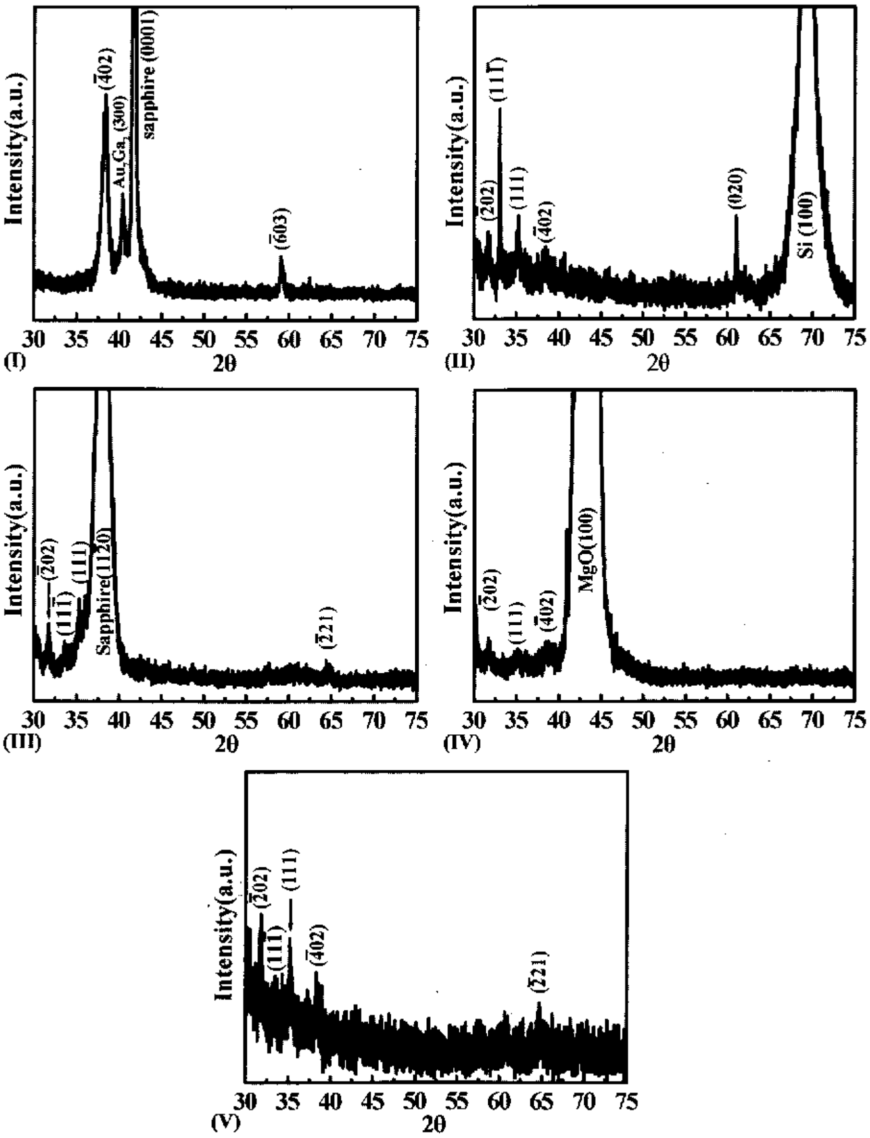

FIG. 3. XRD patterns of Ga_2O_3 nanowires grown on (I) sapphire (0001), (II) Si (100), (III) sapphire (11$\bar{2}$0), (IV) MgO (100), and (V) fused silica substrates at a temperature of 650 °C.

Growth of the Ga_2O_3 nanowires on sapphire (0001) substrates was further conducted at a temperature range of 450–750 °C for 30 min using growth method I. As shown in Fig. 4(a), well-aligned nanowires also formed on sapphire (0001) substrate at 550 °C. When the growth temperature is increased to 750 °C, the well-aligned feature is not observed at all, as shown in Fig. 4(b). Instead, flowerlike nanorod bundles are formed on the sapphire substrate. At a temperature of 450 °C using growth method I, the substrate was loaded at the center of the high-temperature zone; nanowires were not obtained on the sapphire substrate after 30 min growth. Two possible reasons were proposed for the absence of the Ga_2O_3 nanowires on the substrate at 450 °C. One is that the concentrations of Ga and O vapors formed in gas phase at the temperature are not sufficient for the VLS mechanism. The other is that the temperature so low that solution and supersaturation of Ga and O through the Au nanoparticles are limited. To verify this issue, growth of the Ga_2O_3 nanowires was performed in a three-temperature-zone furnace [growth method II, shown in Fig. 1(b)], in which the high-temperature zone (the second zone) was set to 550 °C for acetylacetonate precursor further pyrolysis, but the substrates were loaded in the third-zone region with a temperature of 450 °C. Figure 4(c) reveals that well-aligned nanowires were successfully grown on the sapphire (0001) substrate, suggesting that the absence of the nanowires on the substrate at 450 °C using growth method I is ascribed to the depletion of the O vapor under a pyrolysis temperature of 450 °C. Once sufficient vapors were provided in the gas phase after pyrolsis of the acetylacetonate precursors at 550 °C, the VLS mechanism through the Au catalysts could at a lower temperature of 450 °C for Ga_2O_3 nanowire growth.

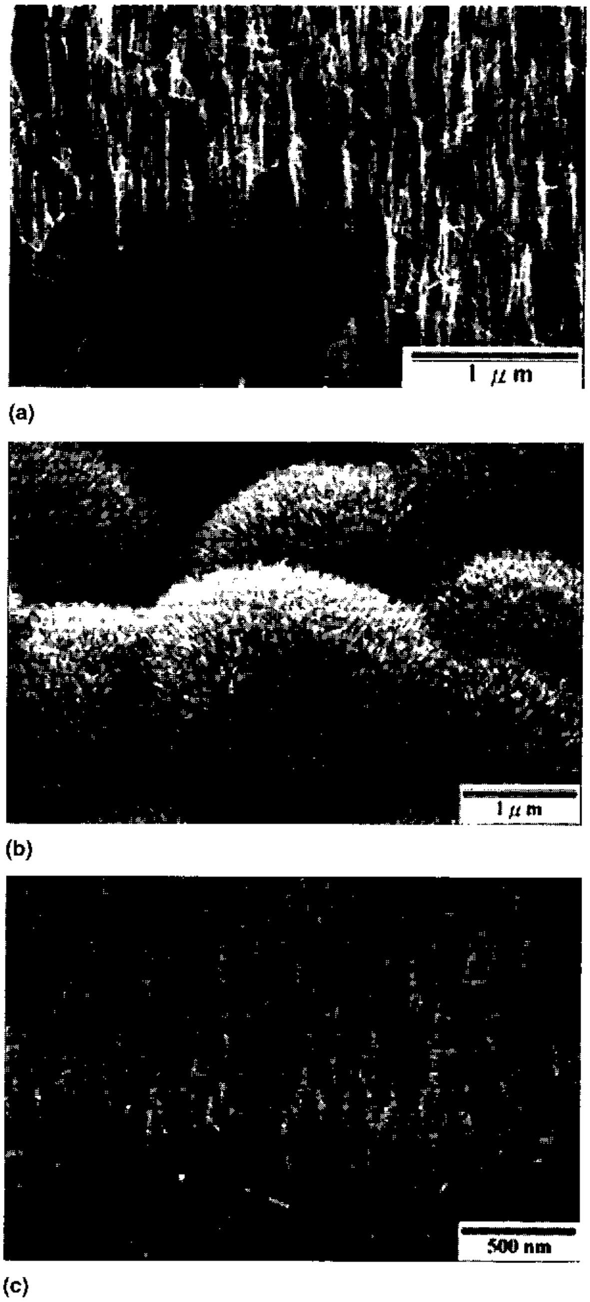

FIG. 4. FE-SEM images of Ga_2O_3 nanowires grown on sapphire (0001) substrate at the temperatures of (a) 550 °C, (b) 750 °C, and (c) 450 °C.

Patterns I–III, represented in Fig. 5, show the XRD patterns of the Ga_2O_3 nanowires grown on sapphire (0001) substrates at 450 (growth method II), 550 and 750 °C (growth method I), respectively. Patterns I and II in Fig. 5 reveal that in addition to the (0001) sapphire diffraction peak, the other two peaks are indexed as the higher-order $(\bar{2}01)$ diffraction peaks of the β–Ga_2O_3

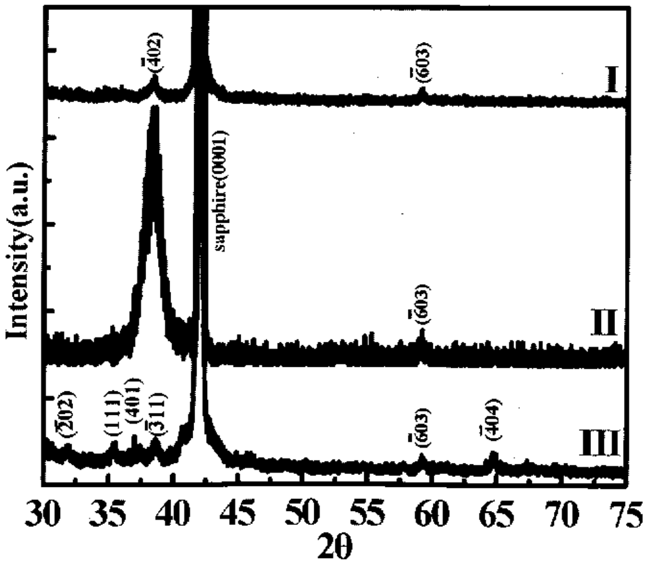

FIG. 5. XRD patterns of Ga_2O_3 nanowires grown on sapphire (0001) substrates at temperatures of (I) 450 °C, (II) 550 °C, and (III) 750 °C, respectively.

structure, demonstrating the nanowires grown on the sapphire (0001) substrates at 450 and 550 °C are preferentially oriented in the $[\bar{2}01]$ direction. Pattern III shows that the diffraction peaks in addition to the one ascribed to the substrate can be indexed to those of β–Ga_2O_3. Preferential orientation of the Ga_2O_3 nanostructures grown at 750 °C on the sapphire (0001) substrate is not observed.

A low-magnification cross-sectional TEM image of the well-aligned Ga_2O_3 nanowires grown on a sapphire (0001) substrate is shown in Fig. 6(a). It reveals that all the nanwires grew in a direction perpendicular to the substrate. The appearance of the nanoparticls on the tops of the nanowires indicates the VLS mechanism for the Ga_2O_3 nanowires growth. A high-resolution TEM image of the Ga_2O_3 nanowires on the sapphire (0001) is shown in Fig. 6(b). The lattice spacing of 0.47 nm corresponds to the d-spacing of $(\bar{2}01)$ planes of β–Ga_2O_3 structure, confirming the XRD analysis that the β–Ga_2O_3 are preferentially oriented in the $[\bar{2}01]$ direction on the sapphire (0001). In addition, the $[2\bar{1}1]$ direction of the Ga_2O_3 nanowires is also parallel to the sapphire $[11\bar{2}0]$ direction. The diffraction patterns of the center β–Ga_2O_3 nanowire, the interfacial region of the Ga_2O_3 nanowire on the sapphire, and the sapphire substrate in Fig. 6(b) taken from fast Fourier transfer (FFT) are shown in Figures 6(c)–6(e), respectively. Figure 6(c) reveals that the β–Ga_2O_3 nanowire possesses a single-crystal structure. Furthermore, Fig. 6(d) indicates that the β–Ga_2O_3 nanowire exhibits an epitaxial relationship with the sapphire (0001) substrate. With the zone axis of [142] and $[1\bar{1}00]$ for Ga_2O_3 and Al_2O_3, respectively, the epitaxial relationship of Ga_2O_3 nanowire and sapphire (0001) is identified: the $[\bar{2}01]$ direction of Ga_2O_3 nanowire aligns with the [0001] direction of sapphire and $[2\bar{1}1]$ direction of Ga_2O_3 nanowire aligns with the $[11\bar{2}0]$ direction of sapphire.

Figures 7(a) and 7(b) show the SEM and backscattering electrons (BE) images of a small flowerlike nanorod bundle formed on the sapphire (0001) substrate at 750 °C after 15-min growth, respectively. The SEM image illustrates that the bundle consists of a lot of branching nanorods. In addition, nanoparticles with an average diameter of 40 nm are dispersed on the surface. The BE image reveals that the nanoparticles are composed of elements with higher atomic number in comparison with those of the nanowires. There is no such nanoparticle on the top of the nanorods. The energy dispersive spectrometry (EDS) of the nanoparticles shows that they consist of Au and Ga. Some twin small bundles are also found on the substrate, as shown in Fig. 7(c). As shown in these images, the bundles originate from a point on the surface, and branching nanorods are developed as they grew up. The flowerlike nanorod bundles were also formed on the

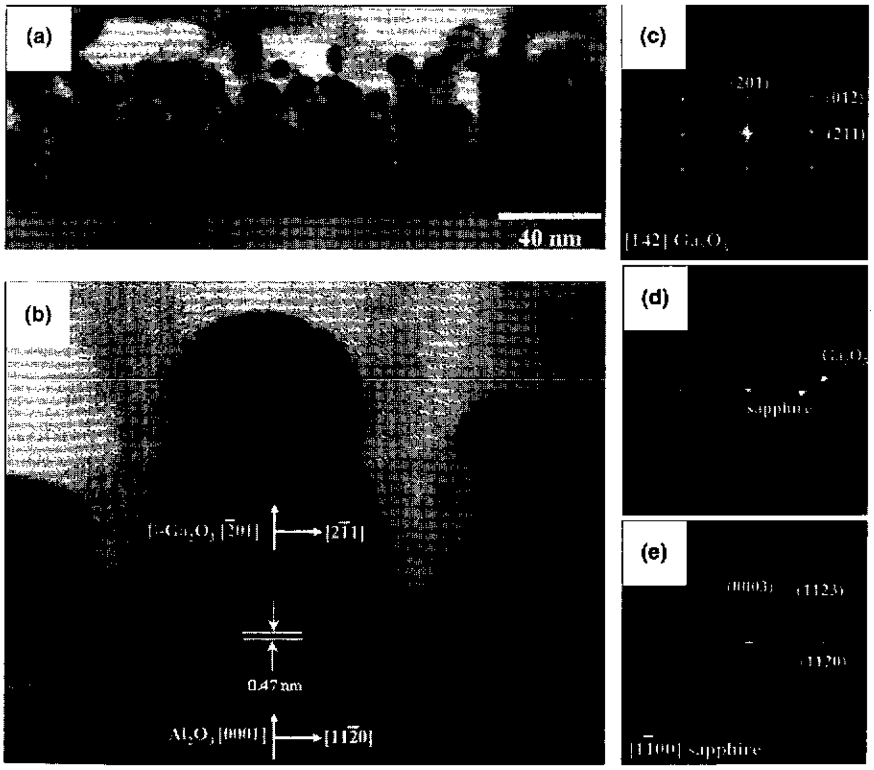

FIG. 6. (a) Low-magnification and (b) high-resolution cross-sectional TEM images of well-aligned Ga_2O_3 nanowires grown on sapphire (0001) substrate and the corresponding diffraction patterns taken from FFT of (c) Ga_2O_3, (d) interfacial, and (e) sapphire (0001) regions.

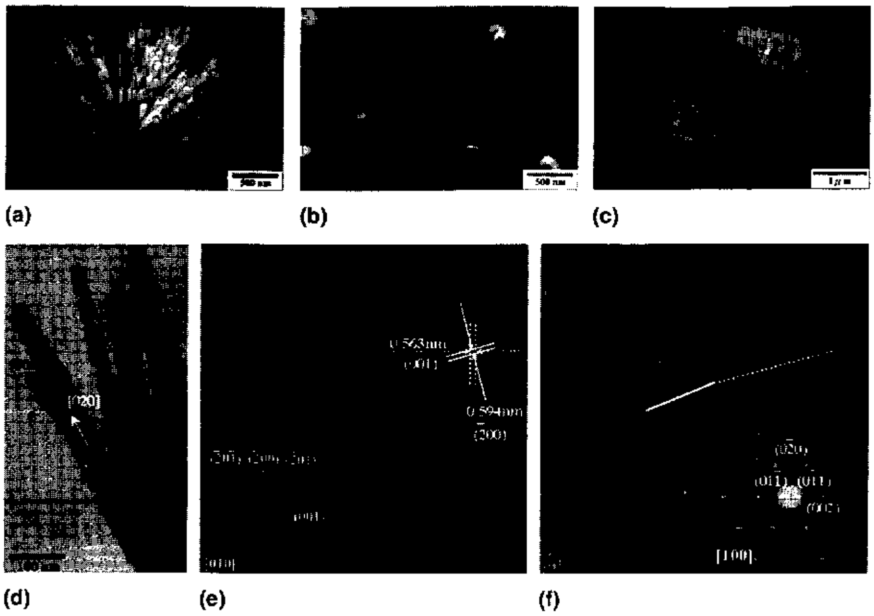

FIG. 7. (a) SEM image and the corresponding (b) BE image of a flowerlike nanorod bundle. (c) SEM image of twin Ga_2O_3 nanorod bundles. (d) TEM image of branching Ga_2O_3 nanorods. (e) HRTEM image of the branch denoted in (d) and the corresponding FFT diffraction pattern. (f) HRTEM image of the junction region denoted in (d) and the corresponding selected-area diffraction pattern.

Au-precoated Si (100) substrate under the same growth conditions. However, nanorod bundles or nanowires were not present when a bare sapphire (0001) was used as the substrate, revealing that the nanoparticles on the surface play a crucial role for the nanorod bundle formation.[15] Structural analyses of the flowerlike nanorod bundles were also performed using TEM. The TEM image of the flowerlike nanorod bundle, as shown in Fig. 7(d), reveals no nanoparticles existing on the top of the nanorods, consistent with the BE analysis. High-resolution (HR) TEM images of a branching nanorod [e region in Fig. 7(d)] and its junction portion [f region in Fig. 7(d)] are shown in Figs. 7(e) and 7(f), respectively. The lattice spacings of 0.563 nm and 0.594 nm shown in Fig. 7(e) correspond to d-spacings of (001) and ($\bar{2}$00) crystal planes of β–Ga_2O_3. The inset of Fig. 7(e), the diffraction pattern taken from FFT, shows the single-crystal structure of the branching nanorod. Figure 7(f) shows the existence of the twin boundary and stacking faults in the junction region, giving rise to each diffraction spot with satellites, as shown in the inset.

Since the nanoparticle is absent on the top of the branching nanorods and it is not possible to grow branching nanorods via the base-growth VLS mechanism[16]—i.e., the catalysts exist at the base of the 1D nanostructures—the formation of the flowerlike nanorod bundles at 750 °C is not believed to follow the VLS mechanism. It has been suggested that a vapor-solid (VS) mechanism would proceed instead of the VLS mechanism when higher vapor pressures of the active species appear in gas phase.[15] In the present work, the flowerlike nanorod bundles are also proposed to be formed via the VS mechanism for higher concentrations of the Ga and O vapors provided at a temperature of 750 °C. The nanoparticles on the surface could play a crucial role to sink the Ga vapor from gas phase to form nuclei suitable for Ga_2O_3 nanorod growth via the versus mechanism. Furthermore, the appearance of the defects in the junction region, as show in Fig. 7(f), suggests that the branching nanorod was grown originating from the defect in the junction.

IV. CONCLUSION

Ga_2O_3 nanowires were grown via the VLS mechanism on various substrates, including sapphire (0001), sapphire (11$\bar{2}$0), Si (100), MgO (100), and fused silica. Well-aligned Ga_2O_3 nanowires were formed only on the sapphire (0001) substrates at temperatures of 650–450 °C. In the case of 450 °C, supplying sufficient O vapor in gas phase through pyrolysis of the acetylacetonate precursor at a temperature of 550 °C is needed for the growth of the well-aligned Ga_2O_3 nanowires on sapphire (0001). Structural analyses reveal that the well-aligned Ga_2O_3 nanowires are expitaxial grown on the sapphire (0001) with Ga_2O_3/ sapphire orientational relationship [$\bar{2}$01]||[0001] and [211]||[11$\bar{2}$0]. In addition, formation of the flowerlike Ga_2O_3 nanorod bundles at a temperature of 750 °C via the VS mechanism was also demonstrated. Instead of being catalysts in the VLS method, the Au nanoparticles play a role in sinking the Ga vapor for forming the nuclei of Ga_2O_3 nanorods in the VS method.

ACKNOWLEDGMENTS

Financial support from the National Science Council in Taiwan under Contract No. NSC 93-2214-E-006-022 is gratefully acknowledged. K.W.C. thanks the Center for Micro/Nano Technology Research, National Cheng Kung University, Taiwan, Republic of China for providing a student scholarship.

REFERENCES

1. M. Ogita, N. Saika, Y. Nakanishi, and Y. Hatanaka: Ga_2O_3 thin films for high-temperature gas sensors. *Appl. Surf. Sci.* **142,** 188 (1999).
2. D.D. Edwards, T.O. Mason, F. Goutenoir, and K.R. Poeppelmeier: A new transparent conducting oxide in the Ga_2O_3–In_2O_3–SnO_2 system. *Appl. Phys. Lett.* **70,** 1706 (1997).
3. Y.C. Choi, W.S. Kim, Y.S. Park, S.M. Lee, D.J. Bae, Y.H. Lee, G-S. Park, W.B. Choi, N.S. Lee, and J.M. Kim: Catalytic growth of β–Ga_2O_3 nanowires by arc discharge. *Adv. Mater.* **12,** 746 (2000).
4. W.Q. Han, P. Kohler-Redlich, F. Ernst, and M. Ruhle: Growth and microstructure of Ga_2O_3 nanorods. *Solid State Commun.* **115,** 527 (2000).
5. C.H. Liang, G.W. Meng, G.Z. Wang, Y.W. Wang, and L.D. Zhang: Catalytic synthesis and photoluminescence of β–Ga_2O_3 nanowires. *Appl. Phys. Lett.* **78,** 3202 (2001).
6. H.J. Chun, Y.S. Choi, S.Y. Bae, H.W. Seo, S.J. Hong, J. Park, and H. Yang: Controlled structure of gallium oxide nanowires. *J. Phys. Chem. B* **107,** 9042 (2003).
7. X.C. Wu, W.H. Song, W.D. Huang, M.H. Pu, B. Zhao, Y.P. Sun, and J.J. Du: Crystalline gallium oxide nanowires: Intensive blue light emitters. *Chem. Phys. Lett.* **328,** 5 (2000).
8. G. Gundiah, A. Govindaraj, and C.N.R. Rao: Nanowires, nanobelts and related structures of Ga_2O_3. *Chem. Phys. Lett.* **351,** 189 (2002).
9. Z.R. Dai, Z.W. Pan, and Z.L. Wang: Gallium oxide nanoribbons and nanosheets. *J. Phys. Chem. B* **106,** 902 (2002).
10. B.C. Kim, K.T. Sun, K.S. Park, K.J. Im, T. Noh, M.Y. Sung, S. Kim, S. Nahm, Y.N. Choi, and S.S. Park: β–Ga_2O_3 nanowires synthesized from milled GaN powders. *Appl. Phys. Lett.* **80,** 479 (2002).
11. Z.L. Wang: Nanobelts, nanowires, and nanodiskettes of semiconducting oxides from materials to nanodevices. *Adv. Mater.* **15,** 432 (2003).
12. Z.W. Pan, Z.R. Dai, and Z.L. Wang: Nanobelts of semiconducting oxides. *Science* **291,** 1947 (2001).
13. L. Fu, Y. Liu, P. Hu, K. Xiao, G. Yu, and D. Zhu: Ga_2O_3 nanoribbons: Synthesis, characterization, and electronic properties. *Chem. Mater.* **15,** 4287 (2003).
14. K.W. Chang and J.J. Wu: Low-temperature growth of well-aligned β–Ga_2O_3 nanowires from a single-source organometallic precursor. *Adv. Mater.* **16,** 545 (2004).
15. J.Y. Lao, J.Y. Huang, D.Z. Wang, and Z.F. Ren: Self-assembled In_2O_3 nanocrystal chains and nanowire networks. *Adv. Mater.* **16,** 65 (2004).
16. C. Bower, O. Zhou, W. Zhu, D.J. Werder, and S. Jin: Nucleation and growth of carbon nanotubes by microwave plasma chemical vapor deposition. *Appl. Phys. Lett.* **77,** 2767 (2000).